

# Large-Scale Analysis and Modeling for Indoor Propagation at 10 GHz

Andréia V. R. Lopes<sup>1</sup> , Iury S. Batalha<sup>1</sup> , Cristiane R. Gomes<sup>2</sup>   
<sup>1</sup>Computation and Telecommunications Laboratory, Federal University of Pará,  
andreia.lopes@itec.ufpa.br; iurybatalha@gmail.com

<sup>2</sup>Institute of Exact and Natural Sciences, Federal University of Pará, cris.ruiz.gomes@gmail.com

**Abstract**— It is essential to establish dominant propagation mechanisms in indoor environments to model propagation loss for 5th generation networks. This work presents, discusses and analyzes the data of measurement campaigns carried out in the 10 GHz band. These data were obtained in two different scenarios: a corridor and a laboratory. The measurement campaigns were conducted with horn-type directional antennas considering vertical, horizontal and cross-polarization modeling under line-of-sight conditions, where horizontal polarization antenna modeling is the differential of this work. The analysis and comparison of Close-In Reference and Floating Intercept models on a large scale are supported by analysis and considering propagation mechanisms such as reflection and diffraction, which includes calculations of optimal propagation exponent values for each of the polarization in each scenario

**Index Terms**— Channel modeling, radio propagation, 10 GHz, 5G Technology.

## I. INTRODUCTION

Millimetric-wave communication is one of the primary candidate technologies for the new fifth-generation mobile technologies – 5G. Being able to provide of providing multi-Gigabit services such as device-to-device communications (D2D) [1], [2], high-definition television (HDTV), and ultra-high-definition video (UHDV) [3], [4]. Today's mobile data providers offer high latency video and rich media content via wireless mobile broadband, the restriction would be on bandwidth shortages, as global broadband communications tend to support only around 700 frequency spectra MHz and 2.6 GHz [5]-[7]. Capacity and bandwidth are crucial wireless challenges [7], [8], recent studies suggest the use of mmWave bands to increase bandwidth and create opportunities for more access channels for wireless communications [9].

According to the METIS (Mobile and Wireless Communication Enablers for 2020) project, the 10 GHz band appears as a priority band for indoor propagation environments [5], showing better performance than higher frequency bands [10]-[12]. The 28-29 GHz, 32-33 GHz, 43 GHz, 46-50 GHz, 56-76 GHz, and 81-86 GHz spectrums are also focal points for mmWave networks. The millimetric-waves characterization and modeling in indoor, corridor environments are some of the most important stages in the development of 5G mobile access networks.

About modeling at candidate frequency channels, we can cite [13] used a statistical distribution for

corridor environments to mathematically model the external ultra-broadband radio channel - UWB. Conducted measurement campaigns at frequencies from 3.6 to 6.3 GHz with an elliptical planar dipole antenna in vertical co-polarization, in five types of corridors with different characteristics, dimensions and morphologies, and presented studies on the descriptive parameters of the channel such as: signal strength received, average excess delay and RMS delay propagation. Each corridor environment was better modeled by the Ricean distribution for the received power in LoS and the Log-normal distribution for the received NLoS power. It's study how a range of corridors can be accurately described by the same statistical model for received power, mean excess delay ( $\tau_{MEAN}$ ) and root mean square (RMS) delay spread ( $\tau_{RMS}$ ), respectively. The average distribution and RMS distribution of  $\tau$  was better modeled by the normal distribution for the LoS and NLoS scenarios. This work is relevant to the mathematical modeling of the UWB external channel survey in internal corridors and may reduce the efforts required to model future variants of internal corridors, since it validates the assumption that a general corridor can be properly described using a pre- determined for the received signal strength.

At [14], he presents measurement campaigns on multiple super high-frequency bands (SHF) and investigated channel characteristics to correct the problem. Channel comparisons at 3 GHz, 10 GHz, and 28 GHz made in a small room environment. He explores the delay as well as the azimuthal direction and elevation characteristics of the channel using a virtual cylindrical arrangement. The results show that not only wall reflection, but also floor and ceiling reflections are significant in the early propagation delay region.

In [15], LoS and NLoS measurement campaigns were conducted with co- and cross-polarization antennas using directional and omnidirectional antennas in the 4.5, 28 to 38 GHz bands in a corridor of the new WCC wireless communication center at the Malaysian University of Technology, whose corridor walls are made of plasterboard and glass. It proposes a new path loss model for the 28 and 38 GHz bands and shows that large-scale loss results can be modeled with good precision from the classic models that use *PLE*.

The work of [16] presents an extensive analysis of the characteristics of the internal ultra-broadband channel based on measurements in corridors in the frequency bands from 3.1 to 5.3 GHz. The analysis considers stationary states and mobility with large-scale modeling with the normal log model for long-length corridors, and also covered the temporal spread of multipath energy characterized by the spread of RMS delay and Medium Excess (MN-EX). It can be applied to characterize the dispersion of the multipath delay, while the parameter defined as Multipath Gain (MG) is calculated to measure the multipath component strength of the UWB channels. The authors show that the correlation between the propagation of RMS delay and MG varies between 0.06 and 0.84 based on in the physical structure of the environment.

In [17], an empirical model was developed to predict the path loss inside a corridor at 5.3 GHz with only the width of the corridor and the distance from regions in LoS, NLoS and the transition region.

The measurements were made in a perpendicular corridor and the model developed from 30 routes

measured in two different locations, with morphologically different corridors. When the receiver is in the LoS region (that is, the same corridor as the transmitter), the loss of the path can be presented by the loss of the free space path. On the other hand, when the receiver is in the NLoS region (that is, a perpendicular corridor), the loss of the path can be expressed in a simple empirical formula. The model developed was more accurate than the models of Recommendation ITU-R P.1238-6 and WINNER.

The propagation characteristics of mmWave were investigated in an internal corridor environment for the LoS scenario at frequencies of 6, 10, 11, 15, 18, 19, 28, 32 and 38 GHz in [18]. The measurements were made with an omnidirectional antenna on the transmitter and a directional antenna on the receiver, and the receiving antenna configured with vertical and horizontal polarization. Large-scale path loss was characterized based on new and well-known path loss models. A general and less complex method is also proposed to estimate the cross polarization discrimination factor (XPD) of the close reference distance with the XPD (CIX) and ABG path loss models with XPD (ABGX) to avoid the computational complexity of minimum mean square error (MMSE). It also analyzed small-scale parameters, such as propagation of the delay in the mean root square (RMS), delay of the medium excess (MN-EX), dispersion factors and parameters of the delay of the maximum excess (MAX-EX) were used to characterize the channel dispersion by multipath.

The modeling presented by [19] analyzes the loss of propagation inside a corridor and inside a computer laboratory at frequencies of 8, 9, 10 and 11 GHz at the Federal University of Pará. Providing a detailed report of measurement campaigns that use directional antennas in conditions of co-polarization (VV and HH) and cross-polarization (VH) in LoS and obstructed line (OLoS) between transmitter and receiver. The measurement data were used to adjust models Close-In, Floating Intercept (FI), Alpha-Beta-Gamma (ABG) and Close-In Frequency (CIF), through the MMSE method for indoor environments. The approximations in relation to the models loss of trajectory on a large scale for frequencies of 8 - 11 GHz show a convergence with the measured data, due to the method used for the optimization of the MMSE in order to determine the parameters of the model.

Analysis of propagation loss in corridors with different morphologies and dimensions is presented in [20]. The measurement campaigns at 10 GHz were conducted in two corridors with different morphologies and modeled after the Close-In (CI) model in the vertical polarization in LoS. It presents a behavioral statistical analysis for the signal received inside the corridors and shows that there is an increase of 2 dB in the propagation loss inside the corridor with concrete walls, demonstrating that the multipath generated by the permissiveness of the material in the environment are directly related to the loss of signal.

In [21] an internal broadband measurement campaign is described in a university building using a broadband MIMO channel receiver with a bandwidth of 400 MHz to 11 GHz. Using cross-polarized and vertical-polarized antennas and horizontal, presents parameters on a large scale, such as path loss, shading, cross polarization power rate, delay propagation and coherence bandwidth, in addition to polarization behaviors. The path gain characteristics for vertical and horizontal polarization are similar,

differing only in NLoS situations for horizontal polarized corridors. The polarization characteristics of path loss, shading, cross polarization root, delay distribution and coherence bandwidth are analyzed. Average power ratio values for cross-polarization were 12.8 dB for vertical-horizontal polarization and 11.6 dB for horizontal-vertical polarization.

Several 11.2 and 14.6 GHz measurement campaigns were conducted by [22] inside a building in Beijing, China. Large and small scale fading characteristics were investigated based on realistic measurements in environments characterized as a corridor, laboratory, offices and a conference room. Based on the measurements, a model of loss of logarithmic distance trajectory and the propagation of the delay in the square of the square root (RMS) and the characteristics of propagation and delay correlation are also discussed.

The work in [23] shows measurement campaigns at 14 and 22 GHz inside a corridor at the University of KwaZulu-Natal under LoS and NLoS conditions. A large-scale dual-slope model is proposed based on measurements to characterize the channel, its validation is proven through the CI model and its parameters are defined by MMSE and a model based on waveguides that assumes the impact of the wave propagation effect inside a corridor.

In [24] a characterization based on measurement at the frequency of 15 GHz is presented for the corridor scenarios. The characterization of the path loss in two different corridors in the Beijing Jiaotong University building in China, and compares the values of the standard deviations of the scenarios for the facilitation of access points. The value of the loss exponent implies the effect of waveguides within the scenario.

Laboratory measurements for characterizing the propagation channel at 15 GHz are presented in [25], which use both directional and omnidirectional antennas in a LoS situation. It uses the method of scanning towards the sound, rotating the directional antenna in stages to collect the impulse response of the channel in the angular domains. Differences in channel characteristics are compared for a directional and an omnidirectional antenna on the transmitter. Finally, a stochastic cluster model is provided based on five laboratory measurements in the event that the omnidirectional antenna is used on the transmitter.

The propagation characteristics at 19, 28 and 38 GHz are investigated in [26] in a corridor. The measurement campaigns were carried out with directional antennas in LoS and NLoS and five path loss models are studied for the environment and the statistical properties such as Power Delay Profile, RMS delay spread and azimuth angle propagation are compared for the studied ranges. For the NLOS scenario, the angle of arrival (AOA) is extensively investigated, and the results indicated that channel propagation to 5G using a high directional antenna should be used in the beamforming technique to receive the signal and collect all the multipath components. from different angles. a specific mobile location.

The main contributions of this article include: i) measurement campaigns in the real world and at different environments; ii) addition of measurements and data modeling for horizontal polarization; iii)

analysis of large-scale models for 5G propagation.

We conducted two measurement campaigns: the first in a corridor and the second in a laboratory room. We analyzed propagated signal loss information in both environments with vertical, horizontal, and cross-polarized antennas. Unlike most modeling studies that usually only include data on vertical co-polarization and cross-polarization, these campaigns also consider the data for spread modeling obtained through horizontally polarized antennas - this is a significant differentiator from our work. Also, the collected data show all signal loss behavior within environments and reveal new results in the literature, with different values in both scenarios.

## II. THE MEASUREMENT CAMPAIGNS

### A. Equipment and Measuring Setup

We used two horn-type directional antennas, manufactured by MCS Industries, with 15 dBi gain, opening beams of 29° horizontal and 29.3° vertical at 1.7 meters from the ground. The transmitter (Tx) is a synthesized Sweeper 83752A from Hewlett-Packard continuous wave signal generator (CW) ranging from 1 to 20 GHz, and the receiver (Rx) is an Anritsu MS2692A signal analyzer.

With fixed Tx in the environments, we configure it to provide a transmit power of 0 dBm for vertical (V-V) and horizontal (H-H) co-biases and 15 dBm for cross-polarization (V-H). Rx is moved along the corridor in 1 meter steps in LoS, ensuring that no person gets in or near the transmitted beam. Table I specifies the equipment and configuration for all relevant measurement campaign parameters.

TABLE I. SPECIFICATIONS AND PARAMETERS OF THE MEASUREMENT CAMPAIGNS

Parameters	Configurations	Units
Central Frequency	10	GHz
Signal Transmission	Continuous Wave	-
Antenna Type	Directional	-
Transmitted Power – VV and HH	0	dBm
Transmitted Power – VH	15	dBm
Antenna Height	1.7	m
Antenna Gain	15	dBi
HPBW Azimuth	29	degrees
HPBW Elevation	29.3	degrees

### B. Measuring Scenarios

The corridor is 15.22 m long and 1.37 m wide. Fixing Tx at 1.3 m from the wall and repeatedly moving Rx away from Tx by 1 m in each interaction, until a distance of 14 m. In this scenario, there are brick walls, smooth concrete floors, and wooden doors. There are also some iron bars and metal boxes for power panels.

The signal analyzer captures 10,001 values of received power in each data collection, and the 10,001 has been collected ten times in each point, resulting in 100,010 data of received power. Having measured 14 points for vertical co-polarization, 10 points for horizontal co-polarization and 8 points for cross-polarization, thus totaling 140,014, 100,010 and 80,008 total received power values, respectively. Totaling 320,032 received power values collected inside the corridor. The measured points difference

is due to diverse values of signal loss as distance increased, resulting in noise-level reception at Rx. Fig. 1 presents the corridor scenario.

The laboratory is 14.97 m long and 7.67 m wide. Fixing the Tx with a difference of 1.3 m from the wall and moving Rx iteratively by steps of 1 m, this time to a distance of 12 m. This room consists of masonry walls and brick walls with glass windows, wooden tables, metal chairs, and various desktop computers, as illustrated in Fig. 2. For the laboratory, we defined a central radial component 3.8 m away from the walls.

Similar to the corridor, the 10,001 power values have been collected ten times at each point. Totaling 100,010 values of power received at each measured point. Thus, for the laboratory, we measured 12 points with a distance of 1 m between them for the three polarizations (V-V, H-H, and V-H) and collected 1,200,120 values of received power for each polarization and 3,600,360 received power values collected inside the laboratory.

In contrast to the corridor scenario, it was possible to collect all 12 points distributed throughout the laboratory for the three polarizations. It is important to note that all transmitted power values are equal here - 0 dBm for vertical and horizontal polarizations and 15 dBm for cross-polarization.



Fig 1. Corridor images, depicting Tx (left) and Rx (right).



Fig 2. Laboratory utilized for the measurement campaign.

Each environment had its scenario studied and measured intending to fix the transmitting equipment and progressively moving the receiving equipment throughout the scenarios. The modeling done in both environments uses the average power received from the points collected at each point, determining the loss of propagation by converting the power received at each point.

We chose both scenarios because of the need to develop loss models that consider multipath propagation in waveguide-like structures (for the corridor scenario) and office rooms (for the laboratory scenario) for future networks.

### III. LARGE-SCALE SINGLE FREQUENCY PROPAGATION LOSS MODEL

Measurement-based path loss models provide much more useful insight into real-time propagation on wireless channels. Most radio propagation models have a combination of analytical and empirical methods. The basis of the empirical approach is curve fitting or analytic expressions that recreate a measured data set. This has the advantage of implicitly considering all propagation factors through actual measurements [22] [23] [27] – [29].

The CI model describes propagation loss through a single parameter, defined by distance, and its equation is given in (1).

$$PL^{CI}(f, d) = FSPL(f, d_o) + 10n \log_{10} \left( \frac{d}{d_o} \right) + X_{\sigma}^{CI} \quad (1)$$

$$FSPL(f, d_o) = 20 \log_{10}(4\pi d_o / \lambda) \quad (2)$$

In which  $FSPL$  is the model constant representing the free-space path loss model at a 1 m distance between Tx and Rx, shown in greater detail in (2). Furthermore,  $d_o$  is the reference distance (1 m),  $PLE$  or  $n$  is propagation coefficient according to distance and  $X_{\sigma}^{CI}$  is a random Gaussian variable with the average value of 0, and standard deviation  $\sigma$  in dB. The PLE values found are distinct for each environment and also for each polarization type. This way, there are six different values adopted by PLE. The CI model has a defined extension for cross-polarization (V-H) loss, named CIX. A loss factor

called XPD is added to the CI model, similar to an attenuation factor caused by floors in a building, as shown in [30][31]. In [27] and [29], the author orients usage of PLE as a constant, measured by V-V polarization in an identical environment to where cross-polarization was applied and added to this value the optimized constant XPD. (3) describes the CIX model.

$$PL^{CIX}(f, d) = FSPL(f, d_o) + 10n \log_{10} \left( \frac{d}{d_0} \right) + X_{\sigma}^{CIX} + XPD \quad (3)$$

The FI, or Alpha-Beta model, is utilized for WINNER II and 3GPP standards (3rd Generation of the Public-Private Partnership) [32][33]. This model requires two parameters and does not consider a physical anchor based on the transmitted power and is similar to (4).

$$PL^{FI}(d) = \alpha + 10\beta \log_{10}(d) + X_{\sigma}^{FI} \quad (4)$$

Where  $\alpha$  is the floating interception in dB, and  $\beta$  is the slope. The Gaussian shadowing with zero average value is represented by variable  $X_{\sigma}^{FI}$  in dB and describes large-scale signal fluctuations on average propagation loss over distance. Similarly, to CI and CIX models, the optimal adjustment is through a solution of  $\alpha$  and  $\beta$  minimizes the standard deviation  $\sigma$  through the Least Squares Method - LSM. The  $\alpha$  and  $\beta$  values are very similar to  $FSPL$  and  $PLE$  of the CI model. That implies that the FI model – mainly used in the 3GPP standard for frequency bands below 6 GHz – could also be implemented with satisfaction in mmWave bands of 5G systems [34]. According to [29][35][36], CI and FI models produce very similar shading standard deviations in mmWave channels outdoors.

It is possible to add in the FI model a loss factor equivalent to XPD, seen in (3). In the modeling made for this article, this value is called  $XPD^{FI}$ , where it performs the same function as the cross-polarization loss factor present in the CI model. The values for  $XPD^{FI}$  were found through LSM, reaching the FIX model presented in (5):

$$PL^{FIX}(d) = \alpha + 10\beta \log_{10}(d) + X_{\sigma}^{FIX} + XPD^{FI} \quad (5)$$

The CI and FI models and their respective extensions are based on fundamental principles of wireless propagation, inspired by Friis and Bullington, where  $\beta$  and  $PLE$  offer an insight on environment-based path loss, with a numerical value of 2 on free space occasions, as shown by Friis [30].

#### IV. RESULTS AND ANALYSIS

In this section, there will be a presentation of results in LoS situations for both environments, utilizing models CI, CIX, FI, and FIX. Besides that, two analyzes will be presented: a comparative analysis for the standard deviation and another between the results presented in this work with the works present in the literature. The parameter that determines the slope size for the models is  $PLE$  and  $\beta$ .  $FSPL$  and  $\alpha$  determine the initial loss for both CI and FI models, respectively.

##### A. Corridor Analysis

For analysis of the models applied to the corridor, Fig. 3 presents the data from the FI model for co-polarizations and the FIX model for cross-polarization, where  $\beta$  represents the slope of the line and

demonstrates how the signal degrades at a distance. It also directly influences the standard deviation values for the measured data in the corridor. The FI model has a good approximation over measured data, because the  $\alpha$  and  $\beta$  values are already predetermined. The values found for  $\alpha$  were 55.54, 60.61, 73.74 and 1.55, 1.64 and 0.08 for  $\beta$  for co-polarization V-V e H-H and for cross-polarization V-H, respectively. For the FIX model, the  $\alpha_{VV}$  data utilized for this modeling represent the optimal value found for vertical polarization propagation.

The value of the cross polarization factor - XPD can also be determined using the MMSE technique such as PLE. It will determine an increase in loss when using cross-polarized antennas.

It is possible to observe that the signal variability is greater in the data in cross polarization, with a variation of almost 10 dB, however the slope is almost linear, that is, the value of the PLE is small. What happens inversely proportional to the data in vertical and horizontal co-polarization, where the variability of the data is less and its PLE value is greater, when compared to the data in cross-polarization. This behavior is seen in both environments.

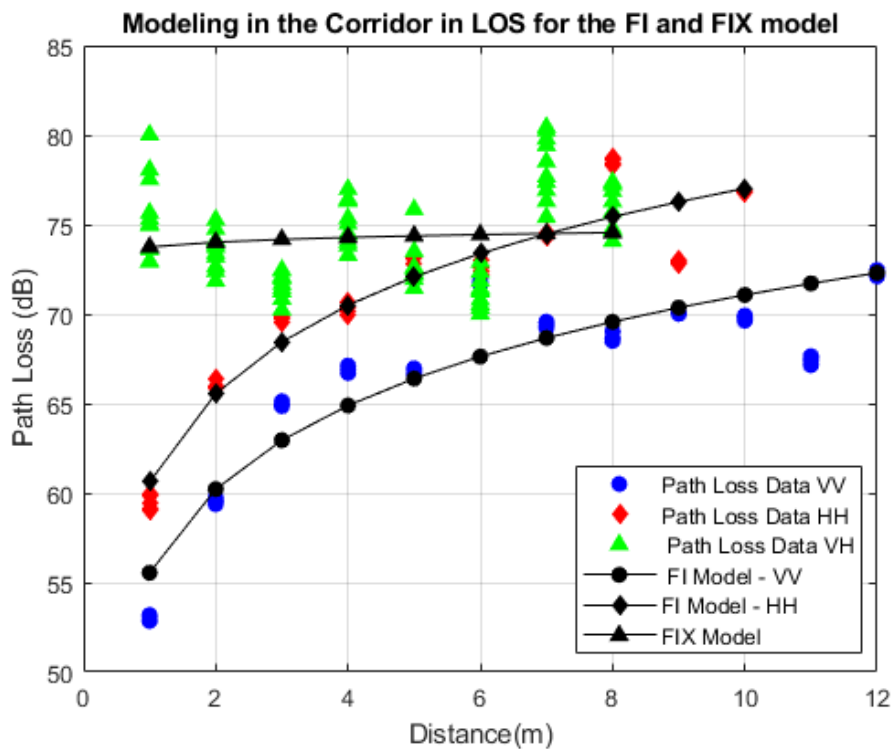


Fig. 3. Path loss data modeled with FI and FIX model for corridor.

Fig. 4 presents signal behavior for the corridor through the CI model for co-polarizations, and CIX for cross-polarization V-H, in which the  $FSPL$  value is the same for co-polarizations, equaling 52.44 dB.

The Close-In propagation loss model is based on the Free Space Equation, which takes into account the wavelength of the propagated signal, thus, the  $FSPL$  represents the physical anchoring of the model. The initial losses are anchored by the  $FSPL$  for the V-V and H-H co-polarizations and the XPD is the

factor that shifts the data in cross-polarizations when added to the FSPL. The PLE values for the CI model were determined using MMSE, with 1.89, 2.66 and 0.08 for V-V, H-H co-polarizations and V-H cross-polarization, respectively.

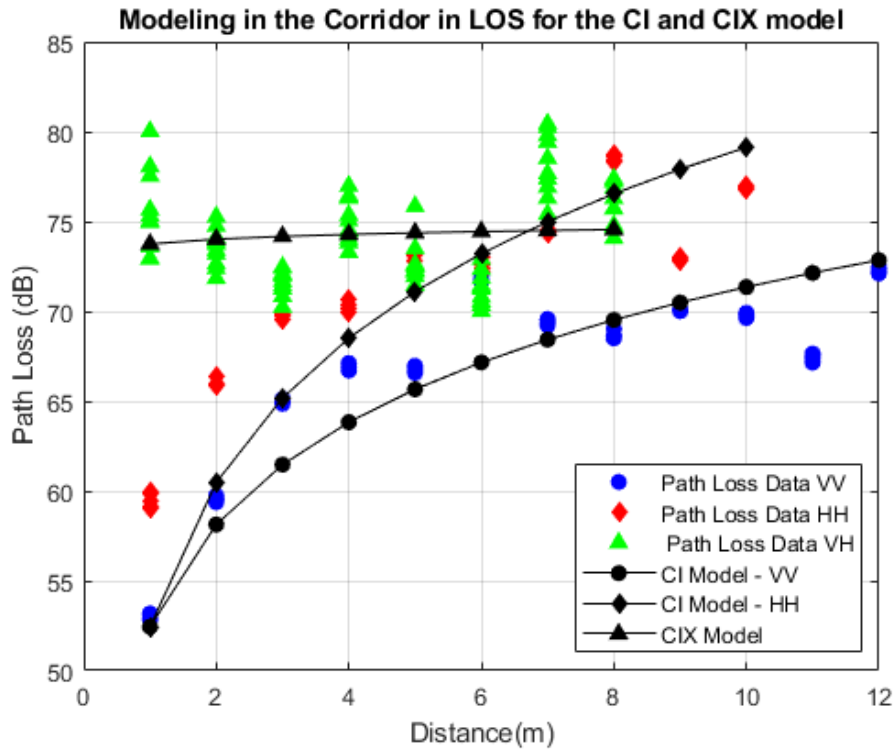


Fig 4. Path loss data modeled with CI and CIX model for corridor.

Table II show the values for  $\alpha, \beta, FSPL, PLE, \sigma$  and  $RMSE$  at models in corridor.

TABLE II. VALUES, IN DB, FOR EACH POLARIZATION IN THE CORRIDOR

Polarization	PLE/ $\beta$	FSPL/ $\alpha$	XPD – CI	XPD – FI	$\sigma$ (dB)	RMSE – FI	RMSE – CI
VV	1.89 / 1.55	52.44 / 55.54	-	-	5.6	1.96	3.67
HH	2.66 / 1.64	52.44 / 60.61	-	-	5.48	1.6	8.33
VH	0.08 / 0.08	52.44 / 73.74	21.3	18.2	2.39	2.22	2.22

The propagation of the signal inside a corridor is still the subject of recurrent studies and investigations in the literature, since they are considered large size dielectric waveguides, with transverse dimensions much larger than the wavelength being propagated inside.

The propagation loss coefficient in waveguides is generally much lower than the loss coefficients in free space and decreases with increasing frequency due to the wave orientation effect.

As mentioned earlier, the standard deviation in the mean of the data in cross-polarization is smaller when compared to the standard deviation of the data in co-polarization, due to the values of PLE and  $\beta$  for the modeling in cross-polarization being smaller in relation to the values of PLE and  $\beta$  in co-polarization. What is shown inversely in the signal variability at each point, with a greater point-to-

point standard deviation for cross-polarization when compared to data in co-polarization. The analysis of the point-to-point standard deviation will be shown later jointly for the two environments.

*B. Laboratory Analysis*

Now, analyzing the models applied to the laboratory, Fig. 5 presents data modeled with FI for co-polarizations V-V and H-H, and FIX for cross-polarization. In which  $\beta$  is the line's slope and represents signal degradation over distance, it also has a direct influence on standard deviation values for measured data in the laboratory. For cross-polarization data, the received loss varies from 70 to 90 dB, with variability diminishing and rising along the line's course.

Under line-of-sight conditions and with radiation diagram in the same polarization there is little variability in received power data, as can be seen in the data measured with blue dots and red dots, V-V and H-H respectively. As it is a more open environment and with walls made of wood-like material, the two co-polarizations show a logarithmic behavior with a loss difference between them of approximately 6 dB. It is possible to denote that the FI loss model has the best approximation over measured data, validating the simulated signal's variability between Tx and Rx, due to the modeling of two fundamental parameters:  $\alpha$  and  $\beta$ .

The  $\alpha$  values found for the laboratory are 53.31, 58.96 and 74.75; and with 1.98, 1.81 and 0.65 for  $\beta$  in the V-V and H-H co-polarizations and V-H cross-polarization, respectively.

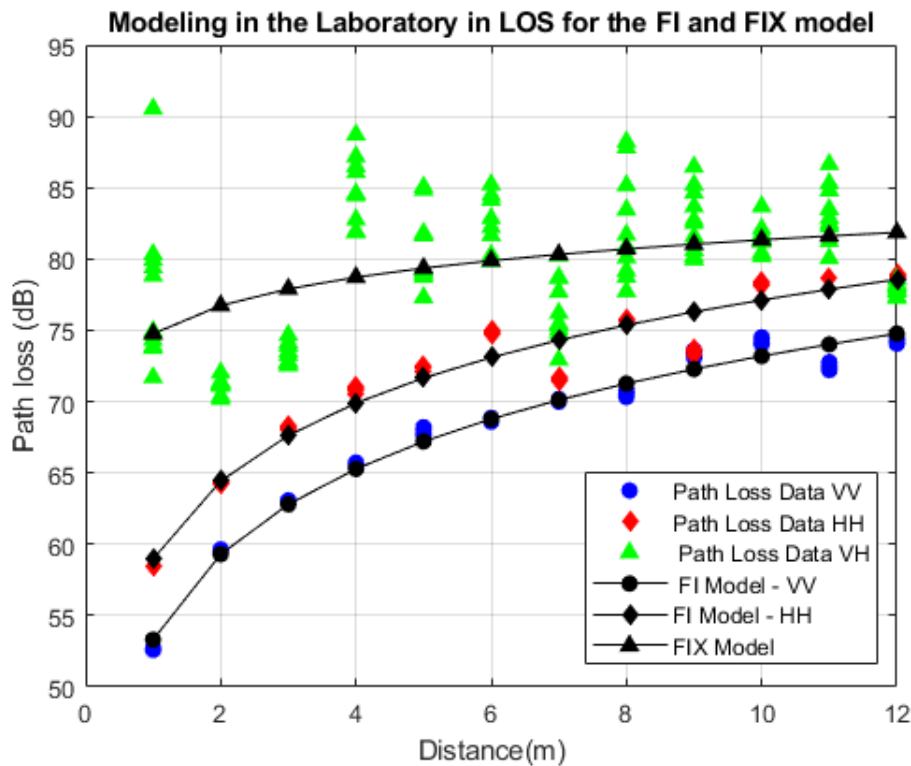


Fig 5. Path loss data modeled with FI and FIX for laboratory.

Still on the laboratory results, Fig. 6 presents modeled signal behavior for through the CI model for V-V and H-H polarizations, and CIX for H-V polarization, although the FSPL value is the same for all three polarization types: 52.44 dB. FSPL values for both environments are, therefore, the same.

The PLE values for the laboratory are different from those found for the corridor, due to the different dimensions and morphologies of the environments. For the laboratory we have 2.08, 2.57 and 0.65 for the V-V and H-H and V-H cross-polarization, respectively.

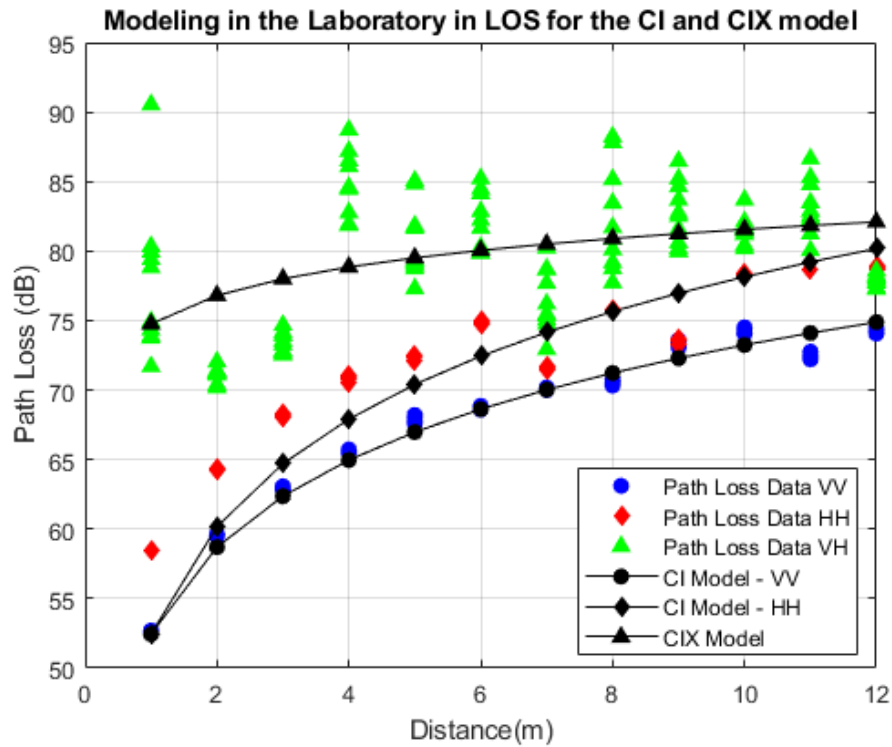


Fig 6. Path loss data modeled with CI and CIX model for laboratory.

As the laboratory environment is wider and more open than the corridor and its composition is made of wood-like material, the attenuation follows an increasing logarithmic trend.

The received power collected inside the laboratory occurred without reaching the noise level up to the point with 12 m between Tx and Rx, and possibly more points would be collected if the environment was longer.

An analysis to be considered concerns XPD in relation to modeling with the CI model within the environments. Since the FSPL value is the same for both environments, as it depends on the wavelength and thus on the frequency of operation. The initial loss for cross-polarization data modeled with the CI model does not come from the FSPL, but from the sum between FSPL and XPD.

The PLE value for the V-H polarization is also an analysis to be considered, as it is lower in comparison to the other co-polarizations.

Table III shows the values of  $\alpha$ ,  $\beta$ , FSPL, PLE,  $\sigma$  and RMSE of the two models for the corridor.

TABLE III. VALUES, IN DB, FOR EACH POLARIZATION IN THE LABORATORY

Polarization	PLE/ $\beta$	FSPL/ $\alpha$	XPD - CI	XPD - FI	$\sigma$ (dB)	RMSE - FI	RMSE - CI
VV	2.08 / 1.98	52.44 / 53.31	-	-	6.56	0.73	1.14
HH	2.57 / 1.81	52.44 / 58.96	-	-	6.12	1.35	6.67
VH	0.65 / 0.65	52.44 / 74.75	22.3	21.4	4.23	3.38	3.49

C. Standard deviation analysis

An important approach in relation to the measured data is to perform a statistical survey using the standard deviation. This analysis shows the extent to which the signal varies from point to point and on average. The point-to-point standard deviation was calculated for this approach in order to determine the signal variation for each meter traveled between Tx and Rx, for co-polarized and cross-polarized environments.

The standard deviation values in the mean for the corridor are 5.6, 5.48 and 2.39, and for the laboratory are 6.56, 6.1 and 4.23 for the V-V and H-H co-polarizations and V-H cross-polarization, respectively. And they are inversely proportional when compared to point-to-point standard deviation values, since the variability of data collected in co-polarization is less than that of data collected in cross-polarization.

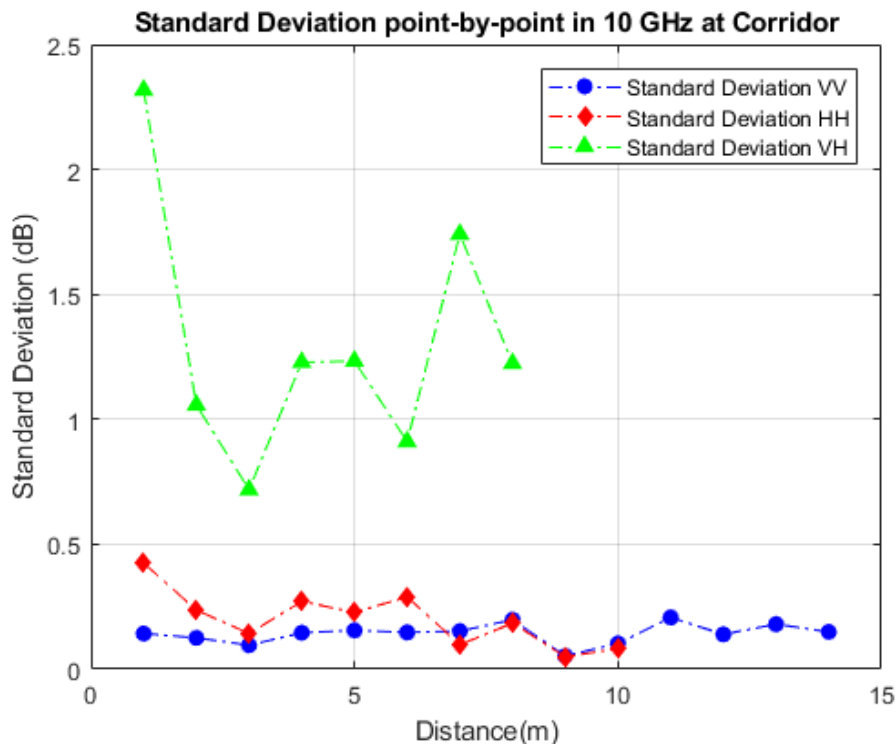


Fig 7. Point-by-point standard deviation analysis for corridor.

Fig. 7 shows the point-to-point standard deviation analysis for the corridor to specify signal variation in the Rx position and for each bias. Blue data (points) show this behavior for the co-polarization V-V, with a low range ranging from 0.10 to 0.20 dB. In red (diamonds), there is data for H-H horizontal polarization ranging from 0.04 to 0.40 dB. Also, the green data (triangles) represent the standard

deviation of V-H cross-polarization, ranging from 0.7 to 2.3 dB.

Total standard deviation values, that is, the values of the standard deviation in the mean, are, therefore, higher for vertical and horizontal polarization compared to cross-polarization modeling. However, the point-to-point standard deviation values for vertical and horizontal polarization are lower than for cross-polarization. The value of PLE is related to this behavior since for cross-polarized antennas, PLE is less than one and greater than 1 for V-V and H-H. Thus, this peer-to-peer statistical analysis is vital to demonstrate the power variability received at each measurement point.

Point-by-point standard deviation data within the laboratory demonstrated in Fig. 8, for signal variation verification for each varying meter of Rx along with the scenario, and all polarizations. Data in blue (dots) show the point-by-point standard deviation for vertical polarization V-V, ranging from 0.04 to 0.24 dB. In red (diamonds), the data for horizontal polarization H-H, in which the point-by-point standard deviation varies from 0.01 to 0.30 dB. Besides, data in green (triangles) represent the standard deviation for cross-polarization V-H ranging from 5.43 to 0.44 dB.

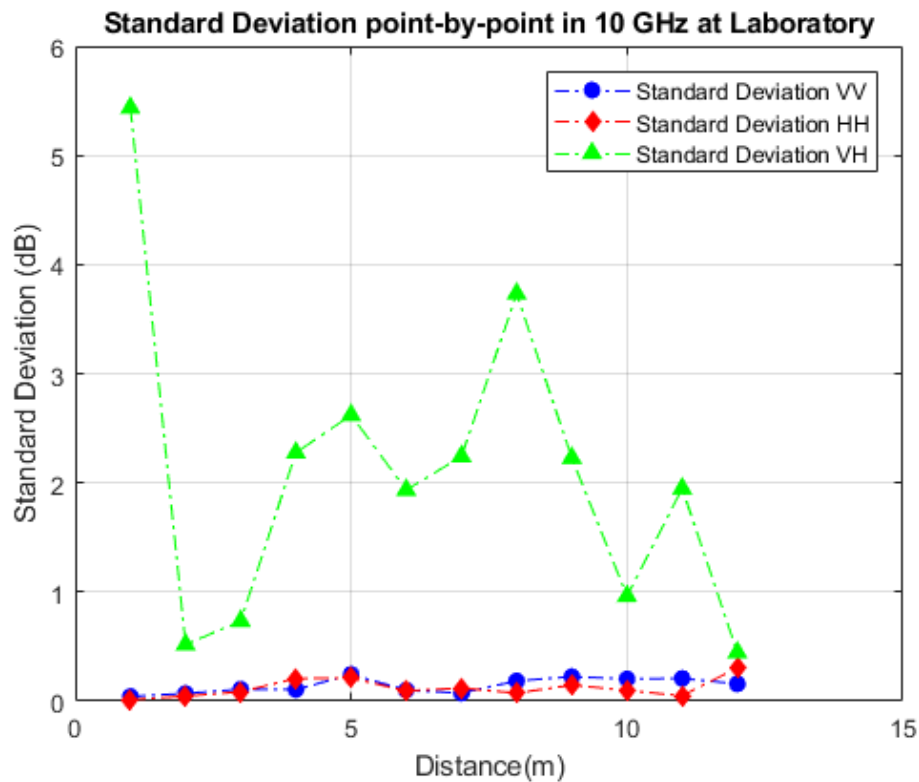


Fig 8. Point-by-point standard deviation analysis for laboratory.

#### D. Analysis and Discussion

Comparing the graphical results for the two environments, we observed that in the laboratory scenario, the received power could be collected at a greater distance if the scenario had a higher width. Meanwhile, for the corridor, the received power was manageable and measurable up until a 14-meter distance between Tx and Rx for vertical polarization, a 10-meter distance for horizontal polarization,



and an 8-meter distance for cross-polarization. We can also conclude that for the three corridor biases, the signal loss is more significant than the laboratory.

The two environments have different propagation characteristics and are composed of different materials. The RMSE values for the corridor are lower compared to the values for the laboratory, due to the influence of spreaders and signal reflecting objects present inside the corridor. Table IV presents the standard deviation and RMSE values for the studied models implemented in both environments.

TABLE IV. STANDARD DEVIATION AND RMSE VALUES FOR EACH POLARIZATION IN THE ENVIRONMENTS

Scenario	Polarization	RMSE – FI	RMSE - CI
Corridor	VV	1.96	3.67
	HH	1.6	8.33
	VH	2.22	2.22
Laboratory	VV	0.73	1.14
	HH	1.35	6.67
	VH	3.38	3.49

The loss of propagation in the corridor followed the behavior of waveguides, while in the laboratory it followed a logarithmic trend. The values of loss inside the corridor are smaller, compared to the values of loss inside the laboratory, because the corridor is a more confined environment than the laboratory, with concrete walls and iron grids, fire extinguishers and other objects at the same height. antennas that generated, possibly, more constructive multipaths. Even with the various objects inside the laboratory, they were below the height of the antennas, and the signal inside the laboratory was not entirely confined, given its wooden walls and glass windows. The analysis of the loss coefficient is widely approached in large-scale modeling at the most varied frequencies, either to validate values already established, or to propose values for new environments and/or frequencies. The study of the PLE for the two environments covered in this work is reinforced by many researchers in the literature, whether in the same method of determination - MMSE - or with algorithms or simulations [15], [17]-[19], [23], [26], [31].

The value of PLE depends on the specific propagation environment, it considers the effects of the propagation channel, and generally assumes that for a given distance between Tx-Rx the loss is the same. The PLE values found for the corridor were 1.89 for V-V co-polarization, 2.66 for H-H co-polarization and 0.08 for V-H cross-polarization.

In the modeling done by [19], the PLE values vary from 1.73 to 2.16 for runners and from 2.07 to 2.28 for a laboratory environment. In [23] the PLE value found for 14 and 22 GHz varies from 1.6 to 1.7 in vertical polarization inside a corridor, with characteristics similar to the corridor studied in this work. It is worth mentioning the use of the CI model for channel modeling. For the 10.5 GHz frequency, the PLE value presented by [26] was 1, in an open corridor and with plaster walls, which validates the treatment of environmental material to influence signal loss. In [21] the value of the PLE presented is 1.5, in vertical polarization in a corridor, a value close to the PLE proposed in this work. A PLE of 2.12

in a corridor was proposed by [17], when studying propagation in a corridor with different dimensions at the frequencies of 5.3 GHz. For 11 and 14 GHz the PLE values proposed by [22] were 1.52 and 1.59 in an environment corridor and 3.06 and 3.76 for an office environment at the frequencies studied. For [24] the proposed PLE value is 1.57, showing the effect of waveguides in the studied corridor. In [15] the PLE values in the LoS scenario were 0.92, 0.9 and 1.07 dB for the polarizations of the direct antennas in VV, VH and V-Omni (vertical polarization of omnidirectional antennas) at 28 GHz, and 2.3, 2.24 and 2.4 dB for the directional antennas polarized in VV, VH and V-Omin at 38 GHz. It is possible to observe the proximity of the PLE values at 10 GHz with the PLE values at 38 GHz corroborating [34], which indicate that the propagation characteristics at frequencies in the SHF range are similar to the propagation characteristics in the EHF range.

## V. CONCLUSION

This paper has presented a large-scale propagation loss modeling analysis based on extensive propagation measuring campaigns within indoor environments with the aid of directional antennas functioning at the 10 GHz spectrum.

The 10 GHz frequency is one of the priority bands for indoor purposes, according to METIS, the agency behind 5G planning in the European Union. This band is within the Super High Frequency (SHF) range, which possesses similar propagation characteristics to the Extremely High-Frequency range (EHF). Thus, it can be considered as a millimeter-wave band, as reiterated by [29][30][37].

Given that the laboratory scenario has a huge area compared to the corridor, the attenuation follows an increasing logarithmic trend. In the corridor, there is similar behavior to propagation within waveguides. Electromagnetic waves propagating inside the laboratory were hardly confined and could be refracted or diffracted due to the glass windows inside. Whose material offers less influence on signal loss.

The analysis shows that, for internal mmWave channels, large-scale propagation loss related to distance can be modeled with no sacrifice of precision, utilizing simple models like CI and FI.

An investigation of constructive and destructive interference is fundamental to comprehend the propagation mechanisms in both environments. Therefore, in future studies, new measurement campaigns shall be conducted for both large-scale and small-scale analysis.

## ACKNOWLEDGMENT

We would like to thank Computation and Telecommunications Laboratory - LCT for providing the equipment to make the development of this paper possible, and the governmental agency Capes for all financial support. This study was accomplished with the support of the Coordenação de Aperfeiçoamento de Pessoal de Nível Superior – Brasil (CAPES) – Funding Code 001, by the Federal University of Para (UFPA).

REFERENCES

- [1] Q. Du et al, "Interference-controlled d2d routing aided by knowledge extraction at cellular infrastructure towards ubiquitous CPS," *Personal and ubiquitous Computing*, vol. 19, no. 7, pp. 1033-1043, 2015. DOI:10.1007/s00779-015-0872-x.
- [2] H. He, Q. Du, H. Song, W. Li, Y. Wang and P. Ren, "Traffic-aware ACB scheme for massive access in machine-to-machine networks," *2015 IEEE International Conference on Communications (ICC)*, London, 2015, pp. 617-622. DOI:10.1109/ICC.2015.7248390.
- [3] M. Elkashlan, T. Q. Duong and H. Chen, "Millimeter-wave communications for 5G: fundamentals: Part I [Guest Editorial]," in *IEEE Communications Magazine*, vol. 52, no. 9, pp. 52-54, September 2014. DOI:10.1109/MCOM.2014.6894452.
- [4] D. Liu et al., "User Association in 5G Networks: A Survey and an Outlook," in *IEEE Communications Surveys & Tutorials*, vol. 18, no. 2, pp. 1018-1044, Second quarter 2016. DOI:10.1109/COMST.2016.2516538.
- [5] Mobile and Wireless Communications Enablers for the Twenty-twenty Information Society (METIS): METIS Channel Models. July 2017, available at: [https://www.metis2020.com/wp-content/uploads/METIS\\_D1.4\\_v3.pdf](https://www.metis2020.com/wp-content/uploads/METIS_D1.4_v3.pdf).
- [6] T. Imai, K. Kitao, N. Tran and N. Omaki, "Radio Propagation for 5G," in *NTT DOCOMO Journal*, vol. 17, no. 4, pp. 40-49, 2017.
- [7] M. N. Hindia, A.W. Reza, K. A. Noordin, M. H. R Chayon, "A Novel LTE Scheduling Algorithm for Green Technology in Smart Grid," *PLOS ONE*, vol.10, no.4, e0121901, 2015. DOI:<https://doi.org/10.1371/journal.pone.0121901>.
- [8] Y. Mo, D. Yu, J. Song, K. Zheng, Y. Guo, "A Beacon Transmission Power Control Algorithm Based on Wireless Channel Load Forecasting in VANETs," in *PLOS ONE*, vol. 10, no. 11, e0142775, 2014. DOI:<https://doi.org/10.1371/journal.pone.0142775>.
- [9] M. Elkashlan, T. Q. Duong and H. Chen, "Millimeter-wave communications for 5G – Part 2: applications [Guest Editorial]," in *IEEE Communications Magazine*, vol. 53, no. 1, pp. 166-167, January 2015. DOI:10.1109/MCOM.2015.7010530.
- [10] A. R. Othman et al, "Modeling of Indoor Wave Propagation Models from 1 G Hz to 10 G Hz," in *4th International Symposium On Broadband Communication - ISBC*, 2010.
- [11] Y. Mo, "Mobile and Wireless Communications Enablers for the Twenty-twenty Information Society (METIS): Intermediate description of the spectrum needs and usage principles," August 2013, available at: [https://metis2020.com/wp-content/uploads/deliverables/METIS\\_D5.1\\_v1.pdf](https://metis2020.com/wp-content/uploads/deliverables/METIS_D5.1_v1.pdf).
- [12] J. Huang, C. Wang, R. Feng, J. Sun, W. Zhang and Y. Yang, "Multi-Frequency mmWave Massive MIMO Channel Measurements and Characterization for 5G Wireless Communication Systems," in *IEEE Journal on Selected Areas in Communications*, vol. 35, no. 7, pp. 1591-1605, July 2017. DOI:10.1109/JSAC.2017.2699381.
- [13] P. A. Catherwood, W. G. Scanlon, "Statistical modeling comparison of wearable UWB signal propagation in antithetical corridor environments," in *IET Microwaves, Antennas & Propagation*, vol. 13, no. 2, pp. 263-268, Feb 2019.
- [14] K. Saito, P. Hanpinitsak, J. Takada, W. Fan and G. F. Pedersen, "Frequency dependency analysis of SHF band directional propagation channel in indoor environment," in *12th European Conference on Antennas and Propagation (EuCAP 2018)*, London, 2018, pp. 1-5. DOI:10.1049/cp.2018.0990.
- [15] M. B. Majed, T. A. Rahman, O. A. Aziz, M. N. Hindia and E. Hanafi, "Channel Characterization and Path Loss Modeling in Indoor Environment at 4.5, 28 and 38 GHz for 5G Cellular Networks," in *International Journal and Antennas and Propagation*, vol. 2018, 9142367, 2018.
- [16] A. M. Al-Samman, T. A. Rahman, M. Hadri, I. Khan and T. H. Chua, "Experimental UWB indoor channel Characterization in Stationary and Mobility Scheme," in *Elsevier Measurement*, vol. 111, pp. 333-339, 2017.
- [17] X. Zhao, S. Geng and B. M. Coulibaly, "Path-Loss Model Including LOS-NLOS Transition Regions for Indoor Corridors at 5 GHz [Wireless Corner]," in *IEEE Antennas and Propagation Magazine*, vol. 55, no. 3, pp. 217-223, June 2013. DOI:10.1109/MAP.2013.6586668.
- [18] A. M. Al-Samman, T. A. Rahamn, M. H. Azmi, M. N. Hindia, I. Khan and E. Hanafi, "Statistical Modeling and Characterization of Experimental mmwWave Indoor Cahnnels for Future 5G Wireless Communications Networks," in *PLoS ONE*, vol. 11, no. 9, p.e0163034, 2016.
- [19] I. S. Batalha, A. V. R. Lopes, J. P. L. Araújo, B. L. S. Castro, F. J. B. Barros, G. P. S. Cavalcante and E. G. Pelaes, "Indoor Corridor and Office Propagation Measurements and Channel Models at 8, 9, 10, and 11 GHz, " in *IEEE Access*, vol. 7, pp. 55005-55021, May, 2019.
- [20] A. Lopes, I. S. Batalha, L. Rocha, F. H. Ferreira, C. G. Ruiz, F. J. B. Barros and A. A. P. Carvalho, "Large-Scale Propagation Modeling in Corridorsat the 10 GHz Frequency Spectrum, " in *2019 SBMO/IEEE MTT-S International Microwave and Optoelectronics Conference (IMOC)*, Nov. 2019.
- [21] M. Kim, Y. Konishi, Y. Chang and J. Takada, "Large Scale Parameters and Double-Directional Characterization of Indoor Wideband Radio Multipath Channels at 11 GHz," in *IEEE Transactions on Antennas and Propagation*, vol. 62, no. 1, pp. 430-441, Jan. 2014.
- [22] X. Zhou et al., "Indoor wideband channel measurements and analysis at 11 and 14 GHz," in *IET Microwaves, Antennas & Propagation*, vol. 11, no. 10, pp. 1393-1400, September 2017. DOI: 10.1049/iet-map.2017.0191.
- [23] N. O. Oyie and T. J. O. Afullo, "Measurements and Analysis of Large-Scale Path Loss Model at 14 and 22 GHz in Indoor Corridor," in *IEEE Access*, vol. 6, pp. 17205-17214, 2018. DOI: 10.1109/ACCESS.2018.2802038.
- [24] B. Zhang, Z. Zhong, X. Zhou, K. Guan and R. He, "Path loss characteristics of indoor radio channels at 15 GHz," in *10th European Conference on Antennas and Propagation (EuCAP)*, Davos, 2016, pp. 1-5. DOI:10.1109/EuCAP.2016.7481177.

- [25] X. Yin, Y. Ji and H. Yan, "Measurement-Based Characterization of 15 GHz Propagation Channels in a Laboratory Environment," in *IEEE Access*, vol. 5, pp. 1428-1438, 2017. DOI:10.1109/ACCESS.2017.2657739.
- [26] A. M. Al-Samman, T. Abd Rahman, and M. Hadri Azmi, "Indoor Corridor Wideband Radio Propagation Measurements and Channel Models for 5G Millimeter Wave Wireless Communications at 19 GHz, 28 GHz, and 38 GHz Bands," *Wireless Communications and Mobile Computing*, vol. 2018, 6369517, 2018. DOI:<https://doi.org/10.1155/2018/6369517>.
- [27] T. S. Rappaport et al., "Millimeter Wave Mobile Communications for 5G Cellular: It Will Work!," in *IEEE Access*, vol. 1, pp. 335-349, 2013. DOI:10.1109/ACCESS.2013.2260813.
- [28] G. R. Maccartney, T. S. Rappaport, S. Sun and S. Deng, "Indoor Office Wideband Millimeter-Wave Propagation Measurements and Channel Models at 28 and 73 GHz for Ultra-Dense 5G Wireless Networks," in *IEEE Access*, vol. 3, pp. 2388-2424, 2015. DOI:10.1109/ACCESS.2015.2486778.
- [29] T. S. Rappaport, G. R. MacCartney, M. K. Samimi and S. Sun, "Wideband Millimeter-Wave Propagation Measurements and Channel Models for Future Wireless Communication System Design," in *IEEE Transactions on Communications*, vol. 63, no. 9, pp. 3029-3056, Sept. 2015. DOI:10.1109/TCOMM.2015.2434384.
- [30] R. R. Skidmore, T. S. Rappaport and A. L. Abbott, "Interactive coverage region and system design simulation for wireless communication systems in multifloored indoor environments: SMT Plus," *Proceedings of ICUPC - 5th International Conference on Universal Personal Communications*, Cambridge, MA, USA, 1996, vol. 2, pp. 646-650 DOI:10.1109/ICUPC.1996.562653.
- [31] T.S. Rappaport, "Wireless Communications: Principles and practice," 3<sup>rd</sup> ed, *Prentice-Hall*, New-Jersey: Upper Saddle River, 2002.
- [32] Winner II Channel Models: Part I Channel Models, September, 2007. Available at: <https://www.cept.org/files/8339/winner2/2020final/20report.pdf>.
- [33] 3rd Generation Partnership Project Technical Specification Group Radio Access Network: Apatial Cahennel Model for Multiple input Multiple Output (MIMO), Release 15. Available at: [https://portal.3gpp.org/desktopmodules/Specifications/ SpecificationDetails.aspxspecificationId=1382](https://portal.3gpp.org/desktopmodules/Specifications/SpecificationDetails.aspxspecificationId=1382)
- [34] T. S. Rappaport, Y. Xing, G. R. MacCartney, A. F. Molisch, E. Mellios and J. Zhang, "Overview of Millimeter Wave Communications for Fifth-Generation (5G) Wireless Networks—With a Focus on Propagation Models," in *IEEE Transactions on Antennas and Propagation*, vol. 65, no. 12, pp. 6213-6230, Dec. 2017. DOI:10.1109/TAP.2017.2734243.
- [35] M. K. Samimi, T. S. Rappaport and G. R. MacCartney, "Probabilistic Omnidirectional Path Loss Models for Millimeter-Wave Outdoor Communications," in *IEEE Wireless Communications Letters*, vol. 4, no. 4, pp. 357-360, Aug. 2015. DOI:10.1109/LWC.2015.2417559.
- [36] G. R. MacCartney, Junhong Zhang, Shuai Nie and T. S. Rappaport, "Path loss models for 5G millimeter wave propagation channels in urban microcells," *2013 IEEE Global Communications Conference (GLOBECOM)*, Atlanta, GA, 2013, pp. 3948-3953. DOI:10.1109/GLOCOM.2013.6831690.
- [37] Z. Pi and F. Khan, "An introduction to millimeter-wave mobile broadband systems," in *IEEE Communications Magazine*, vol. 49, no. 6, pp. 101-107, June 2011. DOI:10.1109/MCOM.2011.5783993.